

01 Sep 1975

Non-Isothermal Mercury Pipe Flow Turbulent Characteristics

T. W. Flaherty

L. L. Eyler

A. Sesonske

Follow this and additional works at: <https://scholarsmine.mst.edu/sotil>

 Part of the [Chemical Engineering Commons](#)

Recommended Citation

Flaherty, T. W.; Eyler, L. L.; and Sesonske, A., "Non-Isothermal Mercury Pipe Flow Turbulent Characteristics" (1975). *Symposia on Turbulence in Liquids*. 5.
<https://scholarsmine.mst.edu/sotil/5>

This Article - Conference proceedings is brought to you for free and open access by Scholars' Mine. It has been accepted for inclusion in Symposia on Turbulence in Liquids by an authorized administrator of Scholars' Mine. This work is protected by U. S. Copyright Law. Unauthorized use including reproduction for redistribution requires the permission of the copyright holder. For more information, please contact scholarsmine@mst.edu.

NON-ISOTHERMAL MERCURY PIPE FLOW
TURBULENT CHARACTERISTICS

T.W. Flaherty, L.L. Eyler, and A. Sesonske
Department of Nuclear Engineering
Purdue University
West Lafayette, Indiana 47907

ABSTRACT

The turbulence structure of fully-developed mercury pipe flow, with and without heat transfer, was studied using hot-film anemometry at Reynolds number of approximately 50,000. Single sensors and slanted multiple sensors were used to obtain the radial distribution of axial fluctuating velocity and temperature quantities. Isothermal data were generally in good agreement with comparable air data indicating similar velocity structure. Temperature intensity data agreed with other data in liquid metals.

Axial and radial turbulent heat flux results were somewhat inconclusive. Spectra and turbulence scales were developed providing a picture of the structure.

INTRODUCTION

Heat transfer in liquid metals has been investigated for some years because of their use in high heat flux applications. The inapplicability of analogy approaches to low Prandtl number fluids has resulted in semi-empirical predictive methods which have generally been satisfactory for design purposes. However, more recently, with the need to accurately model heat transfer in irregular geometries under high heat flux conditions in sodium-cooled reactor accident situations, interest has developed in improved approaches which do not require assumptions regarding eddy transport. Therefore, some investigations of the non-isothermal turbulent structure have been undertaken to help develop a useful background for model development. In addition, such measurements in low Prandtl number fluids are of theoretical interest since the modes of heat and momentum transfer are no longer similar, as is the case in higher Prandtl number fluids.

The transport of fluid momentum in a turbulent flow is governed by the Reynolds equations which can be derived from the classical Navier-Stokes relations as shown by Hinze (1959). The Reynolds equation for

fully developed, steady pipe flow neglecting buoyancy and dissipation terms is

$$\frac{1}{r} \frac{d}{dr} (r \overline{u' u'}) = - \frac{1}{\rho} \frac{d\bar{P}}{dz} + \frac{\nu}{r} \frac{d}{dr} \left(r \frac{d\bar{u}}{dr} \right). \quad (1)$$

A similar equation can be developed for the turbulent transfer of heat for steady, fully-developed constant property flow in a pipe

$$\rho c_p \frac{1}{r} \frac{\partial}{\partial r} (r \overline{u' \theta'}) = -\rho c_p \bar{u} \frac{d\bar{\theta}}{dz} + \frac{k}{r} \left(\frac{\partial}{\partial r} \left(r \frac{\partial \bar{\theta}}{\partial r} \right) \right). \quad (2)$$

In addition to the mean and fluctuation quantities appearing in these equations, other statistical quantities are useful for developing turbulent structure information. The turbulent velocity intensity, $\sqrt{\overline{u'^2}}$, and the turbulent temperature intensity, $\sqrt{\overline{\theta'^2}}$, in non-isothermal flow are helpful in describing flow structure. Other statistical quantities such as micro- and macroscales, autocorrelation coefficients, and spectra of velocity and temperature serve to assist in the definition of flow structure. Axial turbulent heat transport, $\rho c_p \overline{u' \theta'}$, and radial turbulent heat transport, $\rho c_p \overline{u' r' \theta'}$, are useful in interpreting phenomena associated with turbulent flow heat transfer.

Experimental efforts by Rust (1966), Burchill (1970), Kudva (1970), Loos (1971), Jacoby (1972), Kowalski (1974), and others provided much needed data for the description of turbulent transport in liquid metals. These investigators were helpful in determining experimental conditions for this work and provided a basis for the comparison of data.

In a parallel but completely independent effort using the same experimental apparatus, Hochreiter (1974) made a number of the same turbulence measurements as reported in this work. However, data reduction techniques were different, as will be indicated. The two investigations therefore complement one another, and where agreement is achieved, serve to improve the confidence in each.

EXPERIMENTAL SYSTEM AND DATA PROCESSING

The mercury flow system used in this study is shown in Figure 1. The fluid, flowed upward through an electrically-heated test section, a circulating pump, a full-flow filter, downward through a return section used for pressure drop measurements, then through a heat exchanger where it was cooled. The 132 diameter long test section, constructed from 1½-inch, type 304, stainless steel pipe, had a 65-diameter entrance length for velocity development followed by a 67-diameter length heated with a uniform wall heat flux for thermal field development. The traversing mechanism, located at the top of the heated test section as shown in Figure 1, allowed three mutually perpendicular probes to be inserted into the flow with the capability of traversing at least 75 percent of the diameter. All three probes penetrated two pipe diameters upstream to minimize any end effects. Hochreiter (1971) and Flaherty (1974) provide additional equipment details.

A two-channel Thermo-Systems, Model 1050, constant temperature hot-film anemometer system was used in this study. A Model 1040 temperature bridge switch was interconnected with each anemometer channel. When this bridge was in the velocity position, the temperature bridge circuit was bypassed and the anemometer functioned in a constant temperature mode. However, when the switch was in the temperature position, the anemometer channel functioned as an uncompensated, constant current anemometer so that the hot-film sensor acted as a resistance thermometer and sensed only temperature fluctuations in the flow.

The turbulent intensities, both velocity and temperature, were measured with a Thermo-Systems, Model 1060, rms meter which had time constants adjustable up to 100 seconds and a frequency response down to 0.1 Hz (3 db point) at a time constant of 100 seconds. Turbulent velocity and temperature fluctuations were also recorded on a four-channel Precision Instrument Company, Model 6200, FM tape recorder.

The hot-film sensors used in this study were 0.002-inch diameter by 0.040 inch long (designated as - 20 sensors by Thermo-Systems). This particular size proved the most satisfactory in a trial of several sized sensors in an attempt to obtain adequate velocity sensitivity with minimum sensor size.

Axial velocity and temperature measurements were made using a single normal sensor. Radial turbulent heat flux was measured using two parallel sensors, oriented at an angle of 45° to the mean flow direction.

Hill and Sleicher's (1971) k-factor sensor directional sensitivity corrections were applied. The two sensors were separated by about 0.010 inches.

The sensors were calibrated in place. The voltage output as a function of velocity at the centerline was least-squares fitted to a power law expression. Differentiation of the fit allowed the sensor sensitivity to velocity to be determined. Temperature sensitivities were determined similarly from a calibration curve of voltage output versus temperature.

Velocity and temperature fluctuation signals were recorded in the FM mode, then converted to digital time series at a maximum rate of 2000 samples per second per channel in form compatible with the CDC-6500 computer. Autocorrelation coefficients, from which micro- and macroscales were determined, and spectra of the axial velocity and temperature fluctuations were obtained using the digitized data.

The direct-lag method was used for calculation of the coefficients and spectra. This more laborious method was used at the time of this investigation rather than a Fast Fourier Transform approach in order to better determine effects of truncation point range, signal aliasing, and data window type. The coefficient and spectra calculations were done at a 95 percent confidence level using the Tukey data window. The upper frequency limit of the analyses was 1000 Hz, which was determined from the frequency response limitations of the sensor operating in the temperature mode. Digitization rate was determined using the Nyquist criteria.

RESULTS AND DISCUSSION

Axial turbulent velocity fluctuations and temperature fluctuations were measured using a single sensor oriented normal to the mean flow direction. Axial turbulent heat flux results were obtained using single sensor fluctuating data. Radial turbulent heat flux results were obtained using two parallel sensors oriented at an angle of 45° to the mean flow direction.

The use of hot-film sensors in mercury is complicated by poor sensor sensitivity, calibration drift, and response attenuation. These difficulties are discussed in detail by Flaherty (1974) and Hochreiter (1971, 1974).

Velocity Fluctuation Measurements

A single, normal hot-film sensor was used to measure the isothermal axial velocity turbulent intensity at several radial positions. The intensity results, normalized to U^* are shown in Figure 2. The friction velocity, U^* , was calculated based on an experimentally verified smooth pipe friction factor.

Results for two sensor overheats are shown and indicate little variation with overheat of the measured intensities.

Also shown in Figure 2, are the air results of Laufer (1953), Patel (1968), and the mercury results of Hochreiter (1974). Laufer's data are lower than the present results. Excellent agreement exists between the present data and the results of Patel and Hochreiter.

The most significant error in the present data is in the determination of the sensor's sensitivity from the experimentally determined calibration curves. The estimated error in $\sqrt{u_z'^2}/U^*$ is 10%, with the present results and those of Laufer, Patel, and Hochreiter all then within experimental error. The present mercury data therefore indicate a similar isothermal velocity structure as air.

Temperature Fluctuation Measurements

Turbulent temperature fluctuations were measured using the single, normal sensor as a resistance thermometer. The normalized temperature fluctuation intensities for a wall heat flux of 7,300 BTU/(hr-ft²) are shown in Figure 3 with the mercury results of Hochreiter (1974) and Loos (1971). For the normalization, the centerline temperature, $\bar{\theta}_o$, and the wall temperature, $\bar{\theta}_w$, were determined experimentally. The maximum of the temperature fluctuation intensity penetrates much further into the turbulent core than does the velocity intensity. The amount of this penetration is a strong function of Prandtl number, being large for a small Prandtl number flow. The consistency of the present data is indicated by the good agreement with the data of Hochreiter and Loos when weighted by the heat flux ratio. The deviation of the present data near $y/R = 0.5$ may be due to a free convection effect.

Axial Turbulent Heat Flux

Axial turbulent heat fluxes, $\rho_c \overline{u_z' \theta'}$, were evaluated using the modified Kovaszny method (1950). The velocity and temperature intensities presented previously were utilized to determine $\overline{u_z' \theta'}$. The normalized flux, $\overline{u_z' \theta'}/u^* \theta^*$, is shown in Figure 4 along with the ethylene glycol (Pr = 70.8) results of Kudva (1970) and the water (Pr = 5.89) results of Burchill (1970). There appears to be a rough proportionality of the axial turbulent heat flux with Prandtl number.

In using the modified Kovaszny method to determine $\overline{u_z' \theta'}$, accurate values of $\overline{u_z'^2}$ and $\overline{\theta'^2}$ must be known. However, in non-isothermal flow, it is difficult to separate the instantaneous velocity and

temperature response of the hot-film sensor. Since Kudva and Burchill strongly indicate that as Prandtl number decreases, the profiles for isothermal and non-isothermal axial velocity intensities collapse to the same curve, isothermal velocity intensities were used here to determine the axial turbulent heat flux using the modified Kovaszny method.

In Figure 4, comparison of the present data with Hochreiter's results at the same Reynolds number (but different wall heat flux) is of interest. He found that at a heat flux of 3,820 BTU/(hr - ft²), energy associated with axial turbulent transport was being transferred from regions of cooler fluid to regions of warmer fluid (positive $\rho_c \overline{u_z' \theta'}$). The present data at a wall heat flux of 7,300 BTU/(hr - ft²) are all much nearer zero. Also shown in Figure 4 is an estimation of the error propagated through the modified Kovaszny method caused by the estimated error in sensor sensitivity to axial velocity and temperature fluctuations.

Radial Turbulent Heat Flux

Radial turbulent heat fluxes were determined for wall heat flux values of 7,300 and 3,650 BTU/(hr-ft²) at a bulk Reynolds number of 50,000. A parallel, inclined dual sensor configuration was used to obtain fluctuating signals which were digitally processed to determine the radial heat flux, $\rho_c \overline{u_r' \theta'}$.

Accurate values of $\overline{u_z' \theta'}$ and $\overline{\theta'^2}$ were required to evaluate the radial turbulent heat flux. The previously presented "near zero" $\overline{u_z' \theta'}$ values at a heat flux of 7,300 BTU/(hr - ft²) yielded results for $\overline{u_r' \theta'}$ which were without trend and unrealistic, owing to the sensitivity of $\overline{u_r' \theta'}$ to the magnitude of $\overline{u_z' \theta'}$. Similarly, Hochreiter's $\overline{u_z' \theta'}$ data at a heat flux of 3,820 BTU/(hr - ft²) provided extremely high and unrealistic results for $\overline{u_r' \theta'}$. Since the present data $\overline{u_z' \theta'}$ were near zero for all radial positions, $\overline{u_z' \theta'}$ was taken to be zero for the evaluation of the $\overline{u_r' \theta'}$ parameter in this work.

Radial turbulent heat flux results for both heat flux cases are shown in Figure 5 to be less than those of Hochreiter (1974) and Burchill (1970). However, Burchill's data which are for water, would not necessarily be expected to agree with the present mercury data since the Prandtl number difference is large. Hochreiter also considered his results to be higher than expected.

Figure 6 shows a comparison of the experimental radial turbulent heat flux at q_w of 7,300 BTU/(hr-ft²) and a theoretical prediction. The theoretical prediction was obtained by subtracting the conduction term in the energy equation from the integral heat flux.

The conduction term was evaluated using the prediction method of Haberstroh and Baldwin (1968). A comparison of the theoretical prediction of Haberstroh and Baldwin with an experimentally determined conduction term obtained by Kowalski (1974) showed good agreement. The bars represent an estimate of the error in the calculation of the radial turbulent heat flux. This error is largely due to uncertainties in the determination of the sensor sensitivity to velocity and temperature fluctuations. Attempts to reconcile the differences between the predicted and calculated values of $\rho c_p \overline{u' \theta'}$ were not successful. However, the measured turbulent convection terms were found to be of the same order as the conduction contribution to the integral heat flux.

Turbulence Scales

Micro- and macroscales of velocity and temperature were determined using the autocorrelation coefficients obtained from digital analysis of the fluctuation signals. Taylor's hypothesis was used to convert the time correlations $f_u(\tau)$ and $f_\theta(\tau)$ to space correlation, $f_u(z)$ and $f_\theta(z)$. A parabolic curve fit near $z = 0$ was used to determine $(\partial f / \partial z)_z = 0$ and hence the microscales. The macroscales were obtained by integrating the autocorrelation functions.

The isothermal velocity micro- and macroscales are shown in Figures 7 and 8 along with the results of Hochreiter (1971). The limited present results for the macroscale show a general tendency to decrease towards the centerline consistent with Hochreiter's data. The results for velocity microscale are only in fair agreement with the results of Hochreiter. However, the autocorrelation coefficients from which the scales were determined for $y/R = 0.4, 0.6,$ and 0.8 had not gone to zero at the maximum lag of $\tau = 0.4$ seconds, thus the accuracy of the present macroscale data is uncertain.

Temperature micro- and macroscales are shown in Figures 9 and 10 respectively, along with the results of Hochreiter (1971) and Loos (1971). Generally good agreement exists for the microscale results for $y/R \lesssim 0.6$ showing a clear indication of a decrease in microscale as the wall is approached. The magnitude of the microscale should decrease near the centerline since the production region is nearer the wall while a more homogeneous decaying region exists near the centerline. Hochreiter's spectrum-based data do not indicate this trend, though the present data, Hochreiter's time derivative-based data, and the results of Loos behave as expected. The temperature macroscale

results of Hochreiter are consistently higher than the present data. A clear indication of a decrease in macroscale as the wall is approached is seen. This is opposite to the trend of the velocity macroscale results which generally tend to decrease as the centerline was approached. These macroscale data, therefore, show the difference between the velocity and thermal field macrostructure.

Spectral Results

The one-dimensional energy spectra of isothermal axial velocity and temperature fluctuations were obtained from time series analyses of digitally converted signals from the single, normal hot-film sensor. The calculated 1-D spectra at $y/R = 0.4$ and 1.0 , are shown in non-dimensional form in Figures 11 and 12. For the normalization, the Kolmogoroff length scales, $L_k = (\nu^3/\epsilon)^{1/4}$, and time scales, $T_k = (\nu/\epsilon)^{1/2}$, were calculated using the microscales of velocity fluctuation to determine ϵ . Similarly, χ was calculated from the temperature microscales. This method was chosen over the spectral integral method since 2 Hz was the lowest frequency analyzed in the spectrum. A complete tabulation of the length scales can be found in Flaherty (1974).

Good agreement exists between the centerline velocity data of Hochreiter which were analyzed using an analog spectrum analyzer and the present data. The slight departure of these data at $k/k_k \approx 10^{-1}$ might be due to error. Hochreiter's results were found to agree well with the theory advanced by Pao (1965) for $k/k_k \gtrsim 1$. At high velocity spectrum wave numbers, some agreement with the -7 power law was noted.

In determining these isothermal velocity spectra results, no correction was made for sensor length as was done by Hochreiter (1971) who used Pao's (1965) correction model for spectra above $k/k_k \approx 10^{-1}$. At Hochreiter's upper frequency limit (≈ 700 Hz) extrapolation of Pao's model yielded a maximum correction factor of 3. Attenuation of the sensor response caused by a large thermal boundary layer existing around the sensor (see, for example, Lim and Sleicher (1974) and Malcolm and Verma (1973)) was found to be less than 10% at centerline dimensionless wave number (Fig. 11) values less than 0.8, the primary region of the results. Hence, no correction was applied.

The centerline temperature spectrum with q_w of 3,650 BTU/(hr - ft²) agrees well with the results of Hochreiter for q_w of 3,800 BTU/(hr - ft²) with a slight discrepancy near $k/k_k \approx 10^{-2}$. The present data indicate the higher heat flux has forced a

redistribution of thermal energy toward lower frequencies, that is, larger eddies, particularly at the pipe centerline where larger eddies dominate the structure of the flow. This is supported by the temperature macroscale results for the two heat flux cases. At $y/R = 0.4$, there is a lesser heat flux effect at low wave numbers. Temperature spectra tend to decrease more rapidly than predicted either by the theories of Batchelor (1959) or Gibson (1968).

CONCLUSIONS

The isothermal turbulent velocity structure for mercury was demonstrated to be similar to that for other fluids at $Re = 50,000$. However, turbulent temperature intensity results demonstrated that the thermal structure of the non-isothermal flow was not similar to the turbulent velocity structure, and that the magnitude of the heat flux strongly influences temperature intensities.

Although the turbulent axial heat flux was found to be negligible, the turbulent radial heat flux was found to be of the same order as radial conduction and roughly proportional to the wall heat flux.

Micro- and macroscale results obtained from autocorrelation coefficients confirmed that the velocity and temperature structure was different. The velocity macroscale tended to decrease toward the centerline while the temperature microscale increased toward the centerline. Limited velocity microscale results indicated a slight decrease near the centerline while the temperature microscales appeared to peak, then decrease slightly toward the centerline.

Neither velocity nor temperature spectra indicated the existence of a $-5/3$ range. At relatively high wave numbers, all temperature spectra decayed with increasing wave number faster than predicted by Batchelor or Gibson.

ACKNOWLEDGEMENT

The support of the National Science Foundation under Grant GK-35776 is gratefully acknowledged. R. N. Houze, L. E. Hochreiter, and R.V.G. Menon provided valuable assistance and advice during the course of the work.

NOMENCLATURE

c_p	Specific heat	$\frac{BTU}{lb \cdot m \cdot ^\circ F}$
$\hat{E}_1(k)$	One-dimensional kinetic energy spectrum function in wave number space	$\frac{ft^3}{sec}$
f	Friction factor	

$f_u(z)$	Normalized, longitudinal space autocorrelation coefficient for velocity fluctuations	
$f_u(\tau)$	Normalized, longitudinal time autocorrelation coefficient for velocity fluctuations	
$f_\theta(z)$	Normalized, longitudinal space autocorrelation coefficient for temperature fluctuations	
$f_\theta(\tau)$	Normalized, longitudinal time autocorrelation coefficient for temperature fluctuations	
k	Wave number	$\frac{1}{ft}$
k	Thermal conductivity	$\frac{BTU}{hr \cdot ft \cdot ^\circ F}$
L_k	Kolmogoroff length scale	ft
\bar{P}	Time-averaged pressure	$\frac{lb}{ft^2}$
Pr	Prandtl number	
q_w	Wall heat flux	$\frac{BTU}{ft^2 \cdot hr}$
R	Inside radius of the test section	ft
Re	Test section bulk flow Reynolds number	
r	Radial direction in cylindrical co-ordinate system	ft
T_k	Kolmogoroff time scale	sec
t	Time	
U_b	Bulk velocity	$\frac{ft}{sec}$
$\bar{U}_{z,r,\phi}$	Time-averaged velocity in z , r or ϕ directions	$\frac{ft}{sec}$
U^*	Friction velocity, $U^* = U_b \sqrt{f/2}$	$\frac{ft}{sec}$
$u'_{z,r,\phi}$	Fluctuating velocity in z , r or ϕ directions	$\frac{ft}{sec}$
y	Distance from test section wall	ft
z	Axial direction in cylindrical co-ordinate system	ft
α	Thermal diffusivity	$\frac{ft^2}{sec}$
ϵ	Dissipation of turbulent kinetic energy	$\frac{ft^2}{sec^3}$
$\bar{\theta}_0$	Centerline temperature	$^\circ F$
θ'	Fluctuating temperature	$^\circ F$
θ^*	Friction temperature	$^\circ F$
$\bar{\theta}$	Time-averaged temperature	$^\circ F$

$\bar{\theta}_m$	Mixed mean temperature	$^{\circ}\text{F}$	
$\bar{\theta}_w$	Mean wall temperature	$^{\circ}\text{F}$	
λ_f	Microscale of axial velocity fluctuations	ft	
λ_{θ}	Microscale of temperature fluctuations	ft	
ν	Kinematic viscosity	$\frac{\text{ft}^2}{\text{sec}}$	
ρ	Fluid density	$\frac{\text{lb}_m}{\text{ft}^3}$	
τ	Lag time increment		
ϕ	Azimuthal direction in cylindrical co-ordinate system	radians	
λ_u	Macroscale of axial velocity fluctuations	ft	
λ_{θ}	Macroscale of temperature fluctuations	ft	

Kovaszny, L. S. G., 1950, "Hot-Wire Anemometer in Supersonic Flow", J. Aero. Sci., 17, 565.

Kowalski, D. K., 1974, "Free Convection Distortion in Turbulent Mercury Pipe Flow," M.S. Thesis, Purdue University.

Kudva, A. K., 1970, "Structure of Turbulent Velocity and Temperature Fields in Ethylene Glycol Flowing in a Pipe at Low Reynolds Numbers," Ph.D. Thesis, Purdue University.

Laufer, J., 1953, "The Structure of Turbulence in Fully Developed Pipe Flow," NACA-TN - 3266.

Lim, G. B., and Sleicher, C. A., 1974, "The Dynamic Behavior of Hot-Film Anemometers in Liquid Metals," Joint Symposium on Flow: Its Measurement and Control in Science and Industry, Instr. Soc. of American, Pittsburgh.

Loos, R. L., 1971, "Characteristics of Turbulent Temperature Fluctuations in Mercury," M.S. Thesis, Purdue University.

Malcolm, D. G. and Verma, V., 1973, "Dynamic Response of Forced Convection Heat Transfer From Cylinders to Low Prandtl Member Fluids," Proceedings of the 1973 Turbulence in Liquids Conference, Rolla, Missouri.

Pao, V., 1965, "Structure of Turbulent Velocity and Scalar Fields at Large Wavenumbers," Phys. of Fluids, 8, 1063-1075.

Patel, R. P., 1968, "Reynolds Stresses in Turbulent Flow down a Circular Pipe," Rept. No. 68-7, McGill University, Montreal Canada.

Rust, J. H. and Sesonske, A., 1966, "Turbulent Temperature Fluctuation in Mercury and Ethylene Glycol in Pipe Flow," Inter. J. of Heat and Mass Transfer, 9, 215.

BIBLIOGRAPHY

Batchelor, G. K., Howells, I.D., and Townsend, A. A., 1959, "Small-Scale Variation on Convected Quantities Like Temperature in a Turbulent Field," J. Fluid Mechanics, 5, 134.

Burchill, W. E., 1970, "Statistical Properties of Velocity and Temperature in Isothermal and Non-isothermal Turbulent Pipe Flow," Ph.D. Thesis, U. of Illinois.

Flaherty, T. W., 1974, "An Investigation of Non-isothermal Turbulent Pipe Flow of Mercury," Ph.D. Thesis, Purdue University.

Gibson, C. H., 1968, "Fine Structure of Scalar Fields Mixed by Turbulence. II. Spectral Theory," Physics of Fluids, 11, 2316.

Haberstroh, R. D., and Baldwin, L. V., 1968, "Application of a Simplified Velocity Profile to the Prediction of Pipe Flow Heat Transfer," J. of Heat Transfer, May, 191.

Heisenberg, W., 1948, "Zur Statistischen Theorie der Turbulenz," Zeitschrift Fur Physik, 124.

Hill, J. C. and Sleicher, C. A., 1971, Rev. of Sci Instr. 42, 1461.

Hinze, J. O., 1959, Turbulence, McGraw Hill Book Company, Inc., New York.

Hochreiter, L. E., 1971, "Turbulent Structure of Isothermal and Non-isothermal Liquid Metal Pipe Flow," Ph.D. Thesis, Purdue University.

Hochreiter, L. E., 1974, "Turbulent Structure of Isothermal and Non-isothermal Liquid Metal Pipe Flow," Int. J. of Heat and Mass Transfer, 17, 113.

Jacoby, J. K., 1972, "Free Convection Distortion of Forced Convection Temperature and Velocity Profiles in Mercury," M.S. Thesis, Purdue University.

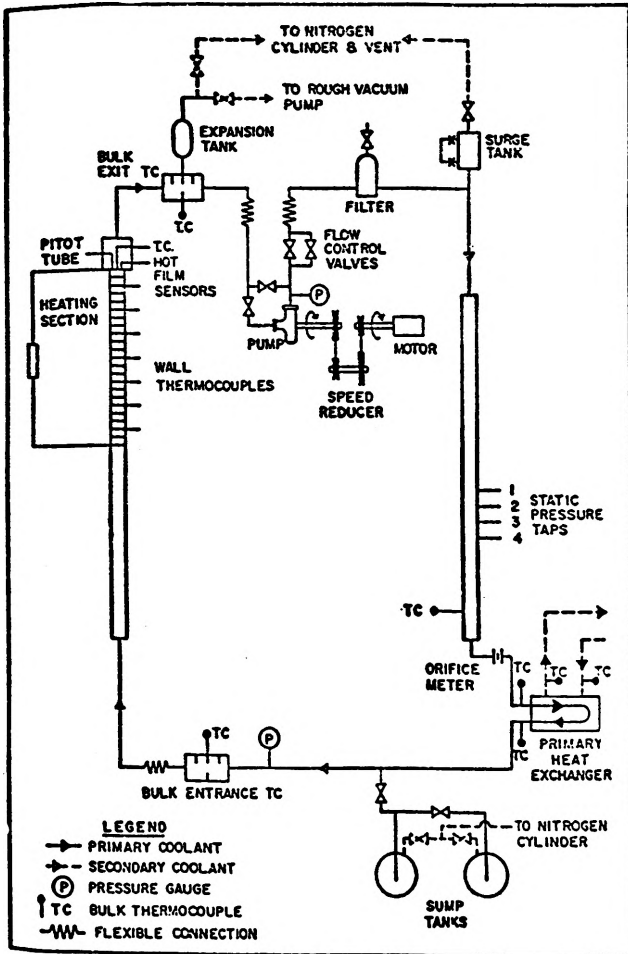


Figure 1. Mercury Heat Transfer Loop.

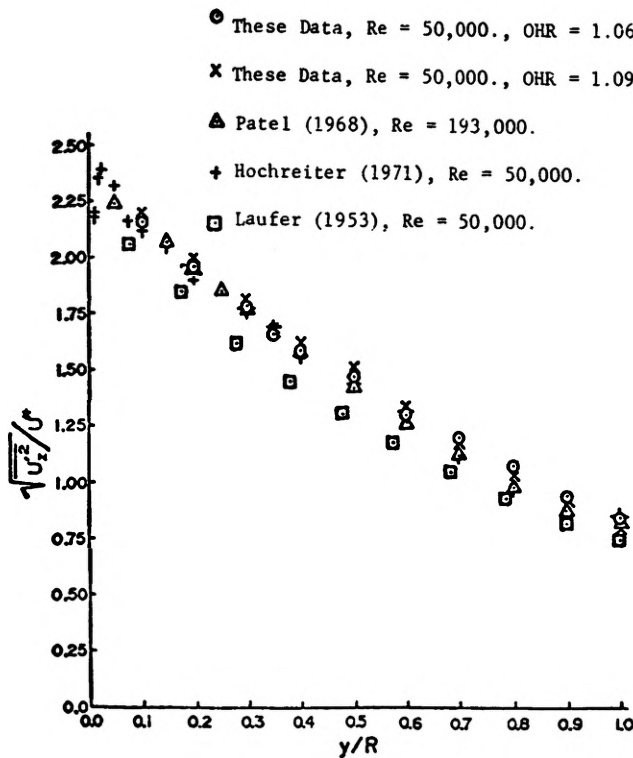


Figure 2. Isothermal Axial Velocity Intensity.

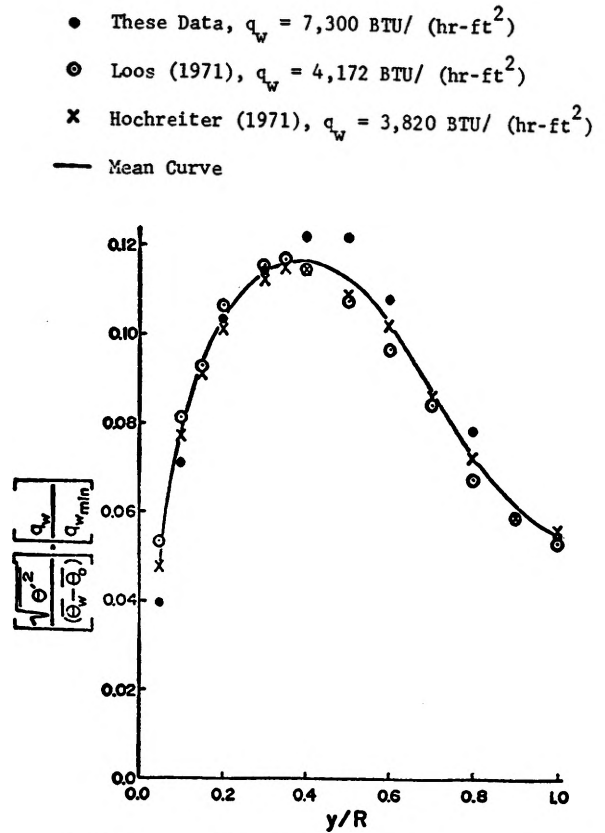


Figure 3. Heat Flux Weighted Temperature Intensities In Mercury At $Re=50,000$.

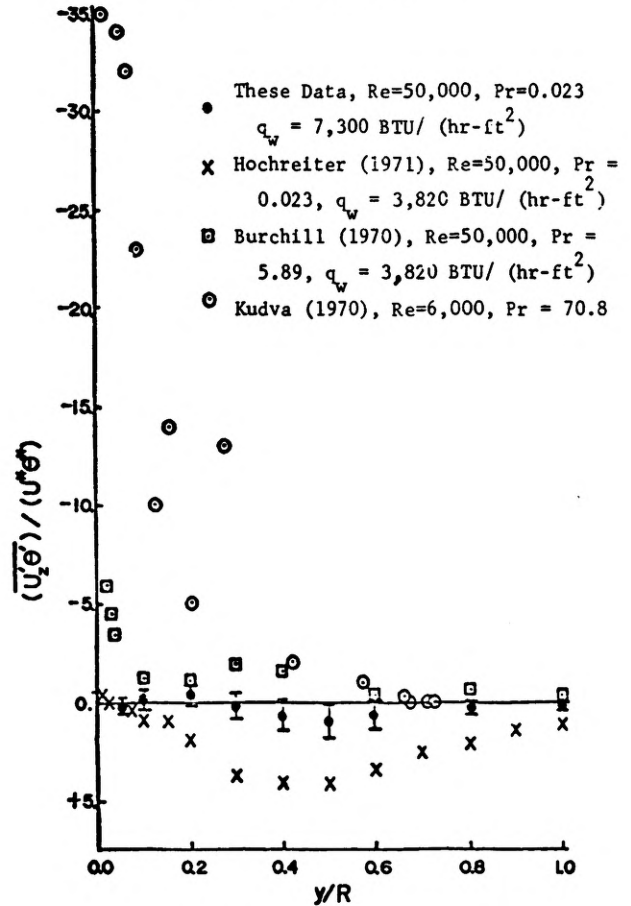


Figure 4. Dimensionless Axial Heat Fluxes.

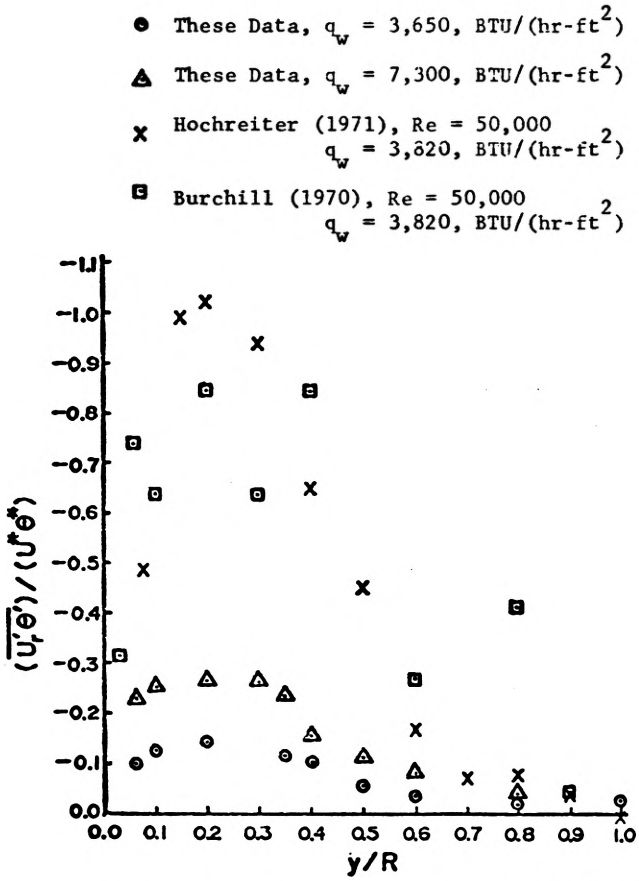


Figure 5. Dimensionless Radial Turbulent Heat Flux Distributions.

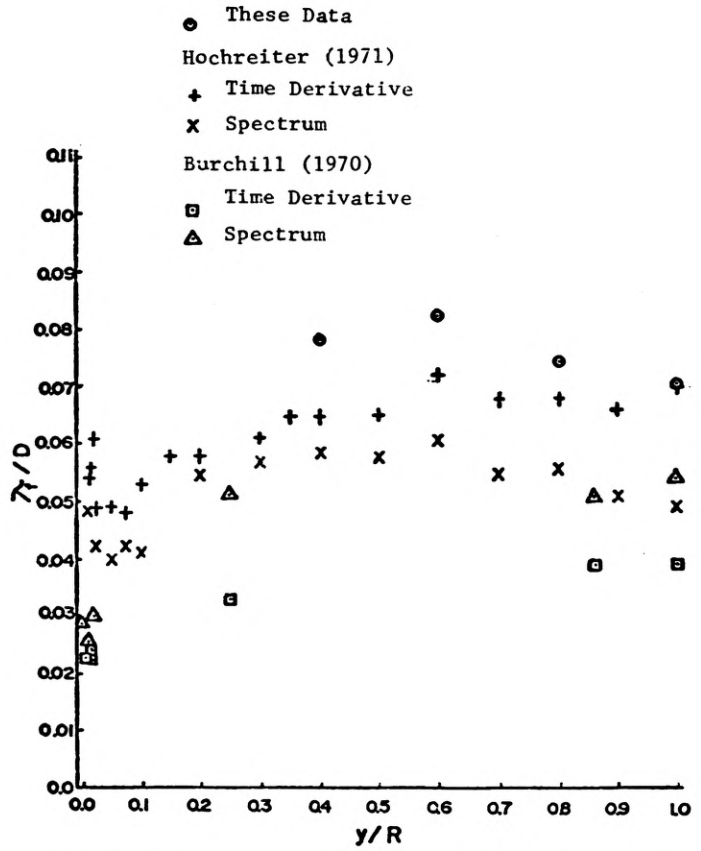


Figure 7. Axial Velocity Dimensionless Microscales.

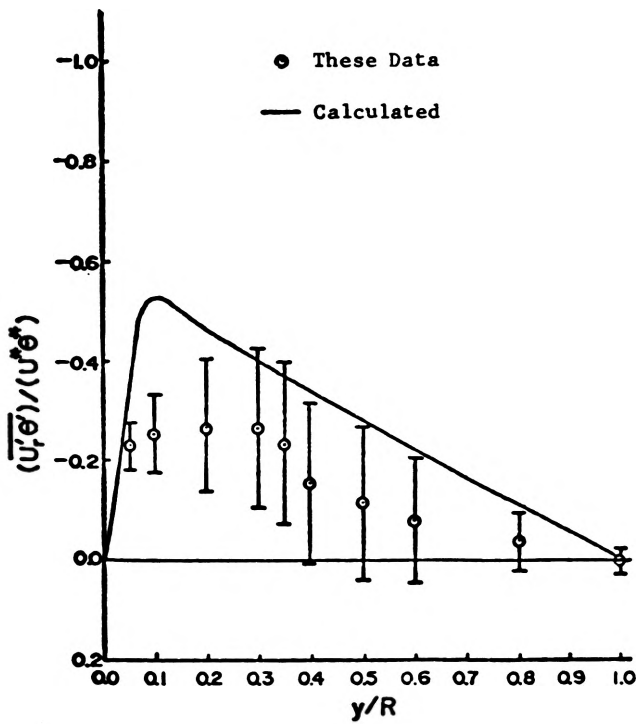


Figure 6. Radial Turbulent Heat Flux Comparison at $q_w = 7,300 \text{ BTU}/(\text{hr}\cdot\text{ft}^2)$.

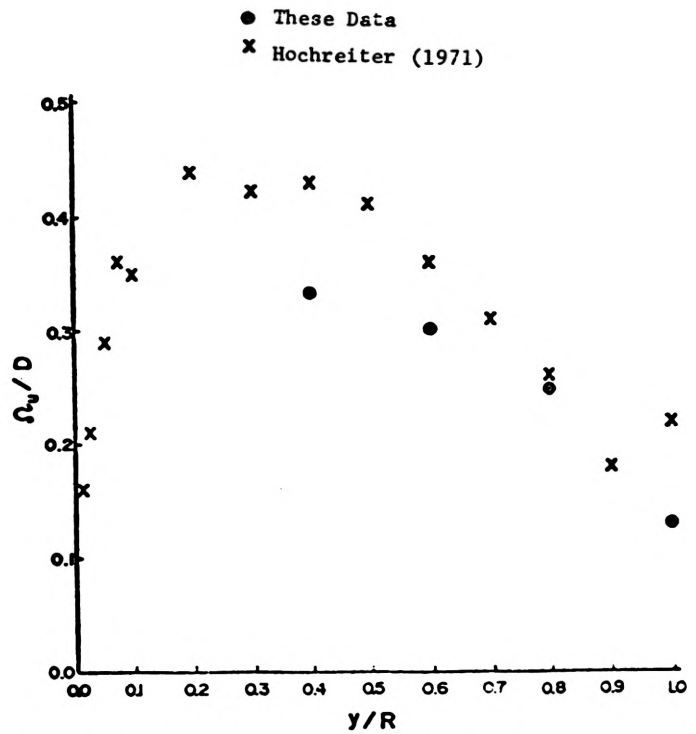


Figure 8. Axial Velocity Dimensionless Macroscales.

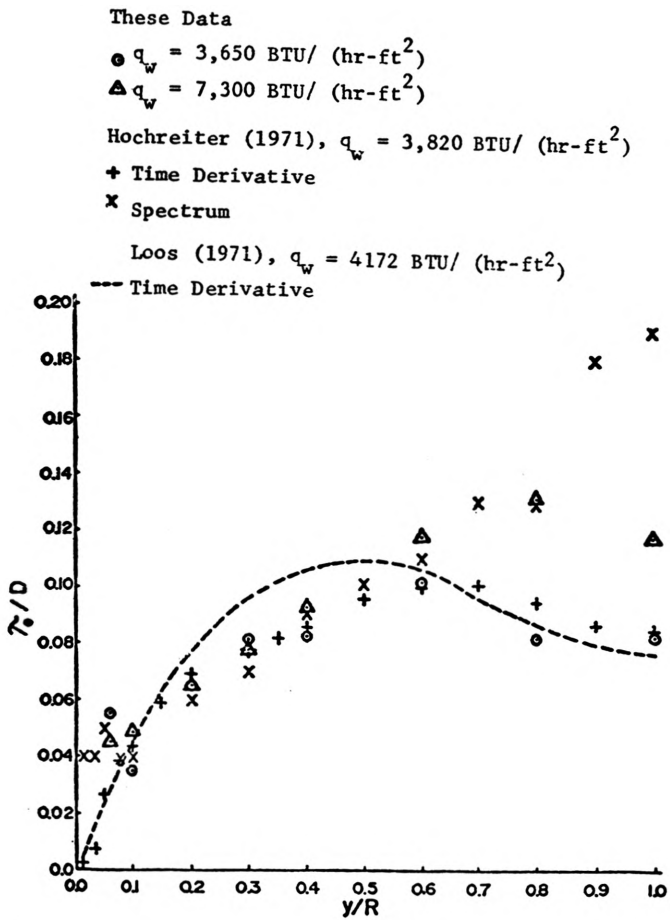


Figure 9. Dimensionless Temperature Microscales.

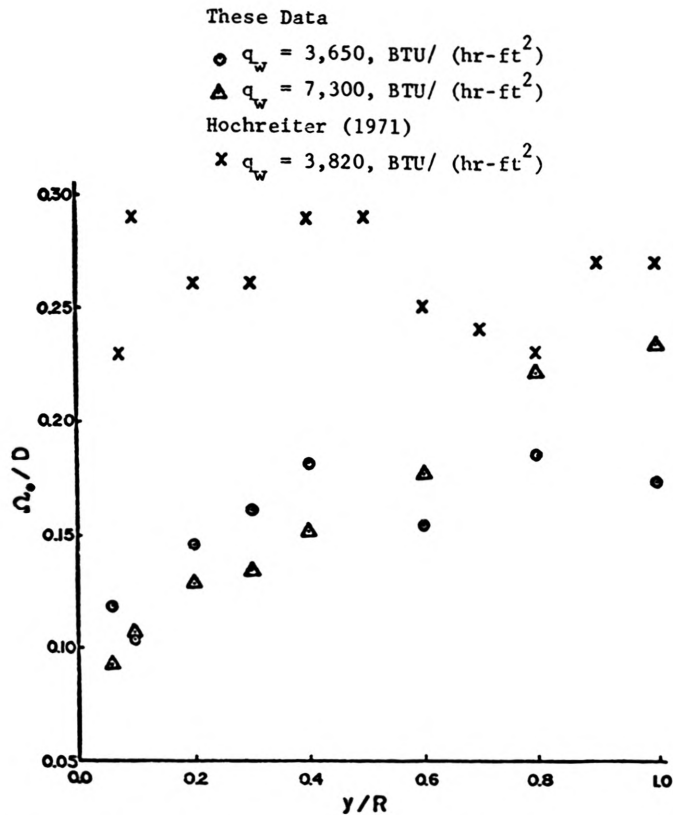


Figure 10. Dimensionless Temperature Macroscales.

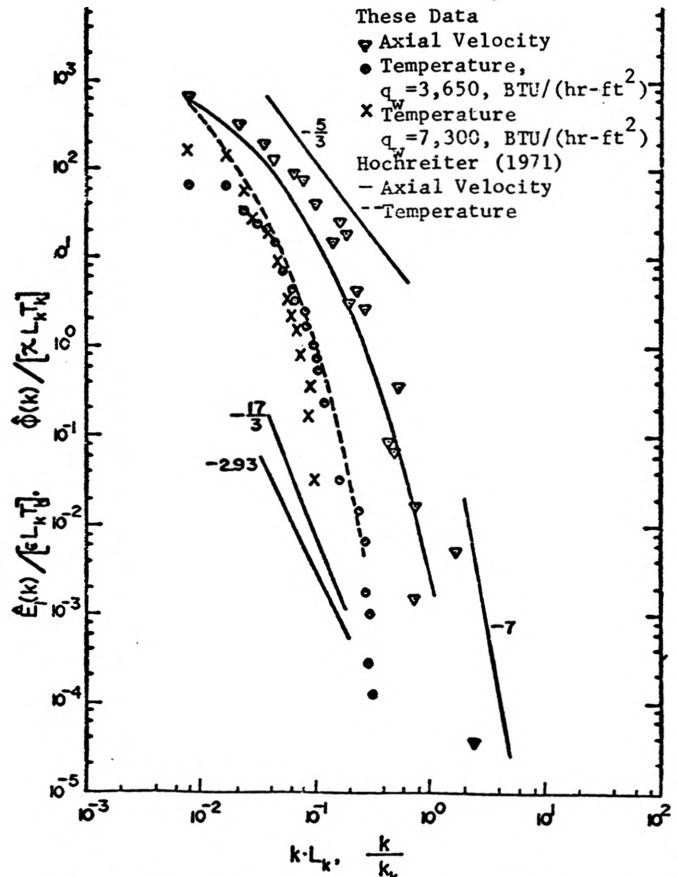


Figure 11. Dimensionless Spectra of Axial Velocity And Temperature At $Y/R = 1.0$.

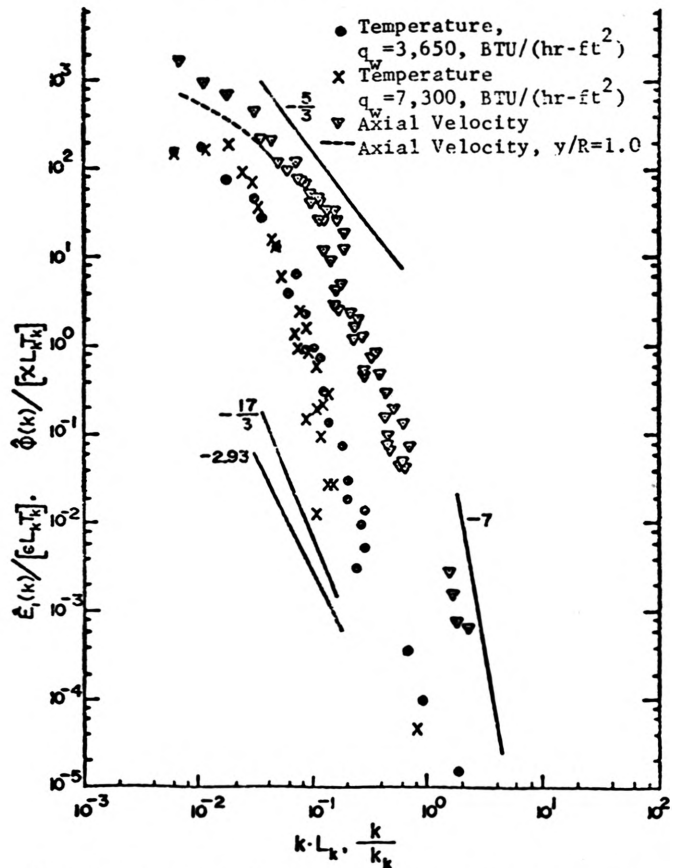


Figure 12. Dimensionless spectra of Axial Velocity And Temperature At $Y/R = 0.4$.

DISCUSSION

Barclay Jones, University of Illinois: I'm interested in your paper because it relates closely to some of the water work that we've been doing recently. In your paper you suggested that you could use the mean velocity as the convection velocity. Our Figure A confirms that the Taylor hypothesis is reasonable. What we show here is the temperature and axial velocity component where we made two point space-time correlations with axial separation and calculated the convection velocity. These results were obtained in water, in the same apparatus Burchill used.

In Figure B we show the frequency behavior of the two velocity components, the normal and the axial (in this case the normal is radial). In comparison to temperature we find that as we approach the wall the frequency component of the normal velocity is much higher than is the axial component. We find that the temperature field agrees closely with the axial component in terms of frequency content. This points out the different influences of the radial and axial velocity components on the temperature structure.

In Figure C we show the integral length scales with respect to radial position. We can see the shift as we pass from the wall to the center line. The normal velocity component length scale rises throughout this region as does the axial velocity component length scale, but the temperature field like the normal velocity near the wall shifts toward the axial velocity structure as you approach the center line and isotropy.

Figure D shows the integral time scales and again we see that near the wall the axial velocity and the temperature scales agree rather closely and as you approach the center the temperature scale moves more toward the normal velocity scale. I think this speaks to the points that you were raising in showing differences across the radius of the tube but with only the axial and temperature field structure available to you. These data are included in the Ph.D. thesis of J. S. Cintra, Jr. ("Experimental and Modeling Studies of Two-Point Velocity and Temperature Fields in Turbulent Pipe Flow," University of Illinois, October, 1975) and show the trends of the temperature structure lying between those of the axial and radial velocities as is expected for a passive scalar.

A. K. M. Fazle Hussain, University of Houston: You indicate that the probe tip was inserted from the end

two-diameters upstream in order to eliminate the exit effect. I have for some time been concerned about the upstream effect of the exit on the turbulent structure. What basis do you have for assuming that at two diameters upstream the exit effect is negligible?

L. L. Eyler, Purdue University: We were guided by the work of Gardner and Lykoudis (J. Fluid Mech., 47, 737 (1971)) who confirmed the linearity of the pressure drop near the end of a similar mercury test section. Now as far as the temperature end effects are concerned, we were guided by several people who have done work in air such as C. J. Lawn (Cent. Elec. Gen. Bd. Report RD/B/N2159, Berkeley, U.K., 1972). However, we do not have thermocouple data for the axial gradient to verify that we are far enough upstream.

Hussain: The mean wall static pressure gradient can at best be an indication of the mean flow field. Thus even if the axial wall static pressure is linear, I remain unconvinced that the effect of the exit on the details of the turbulence structure is negligible at two diameters upstream from the exit.

Eyler: L. G. Genin, et al. (High Temp., 12, #3, 550 (1974)) in Russia, measured the actual turbulent temperature intensity in mercury as a function of axial position. Although the turbulent temperature intensity dropped off at the exit of the tube, the effect was only significant very close to the wall.

Hussain: It would be necessary to look at the detailed hydrodynamic turbulence quantities and I suspect there will be some influence on them as the flow would anticipate the presence of the pipe exit before the flow reaches the exit.

Linden Thomas, Akron University: More and more interest is being given lately to the burst phenomena. It would be interesting to make measurements of the periodicity for liquid metals. Have you given consideration to making such measurements and how would you make them?

Eyler: Well, no, I haven't given any consideration to measuring burst phenomena and I would hesitate to even speculate on what the results would be.

John Laufer, University of Southern California: I would just like to comment on the question of

similarity between velocity fluctuations and temperature fluctuations, comments relevant to Professor Jones' measurements. This question has bothered us for a number of years and a large number of experiments showed gross similarity between axial velocity fluctuation and temperature under certain conditions. The fact that one is scalar and the other a vector quantity complicates the problem. I would like to mention a beautiful piece of experimental work (Ph.D. thesis)

done by Dr. Fulachier at Marseille in a turbulent boundary layer. His measurements of spectral distributions of T' , u' , v' and w' show that in certain regions of the spectrum there is similarity between u' and T' and in other regions of the spectrum between v' and T' and the frequency or wave length over which the similarity occurs changes depending on the position you are in, in the boundary layer.

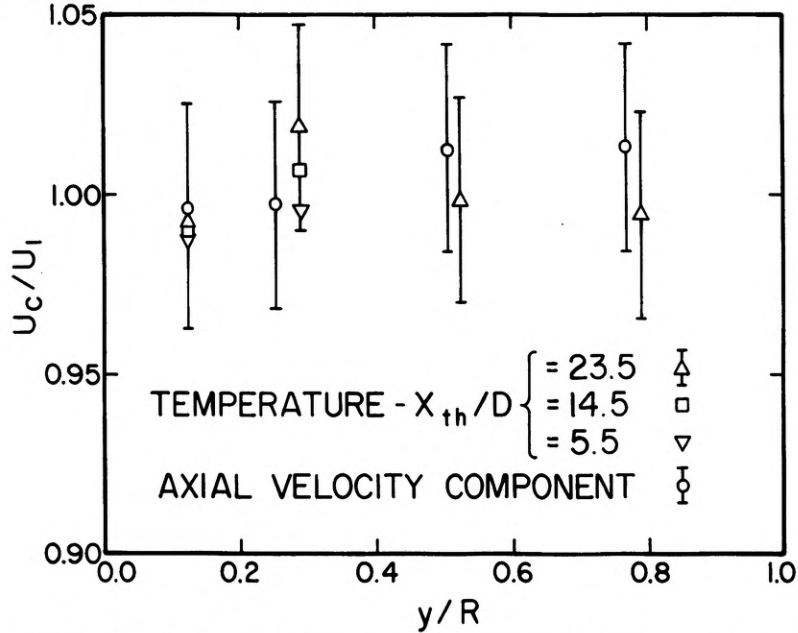


Figure A: Normalized Convection Velocities for Temperature and Axial Velocity Component in Turbulent Pipe Flow.

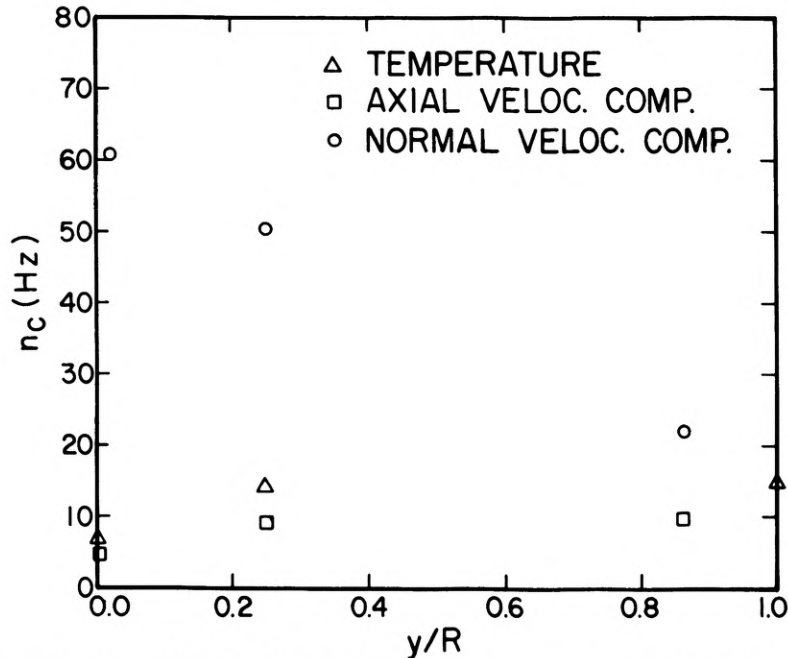


Figure B: Characteristic Frequencies of Temperature and Velocity Component Fluctuations in Turbulent Pipe Flow. (n_c = frequency corresponding to maximum energy of spectral distribution)

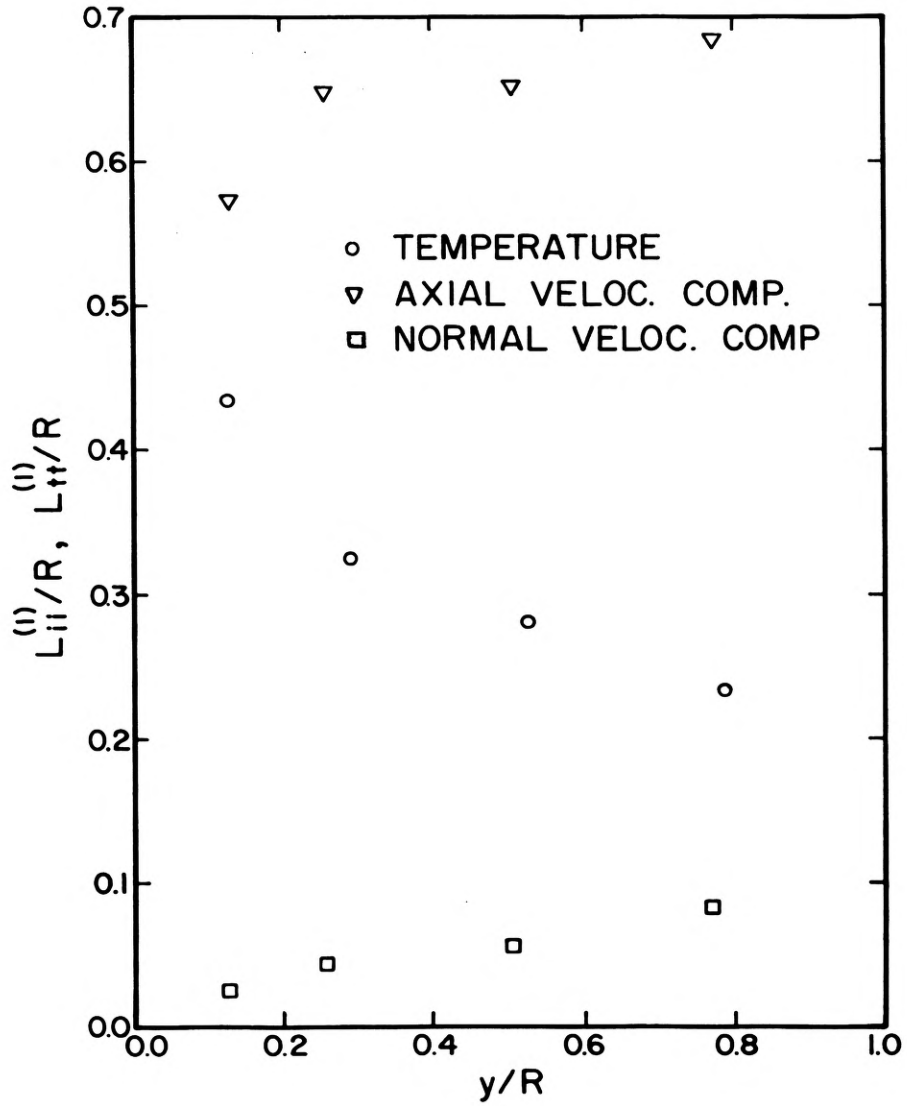


Figure C: Integral Axial Length Scales for Velocity Components and Temperature in Turbulent Pipe Flow

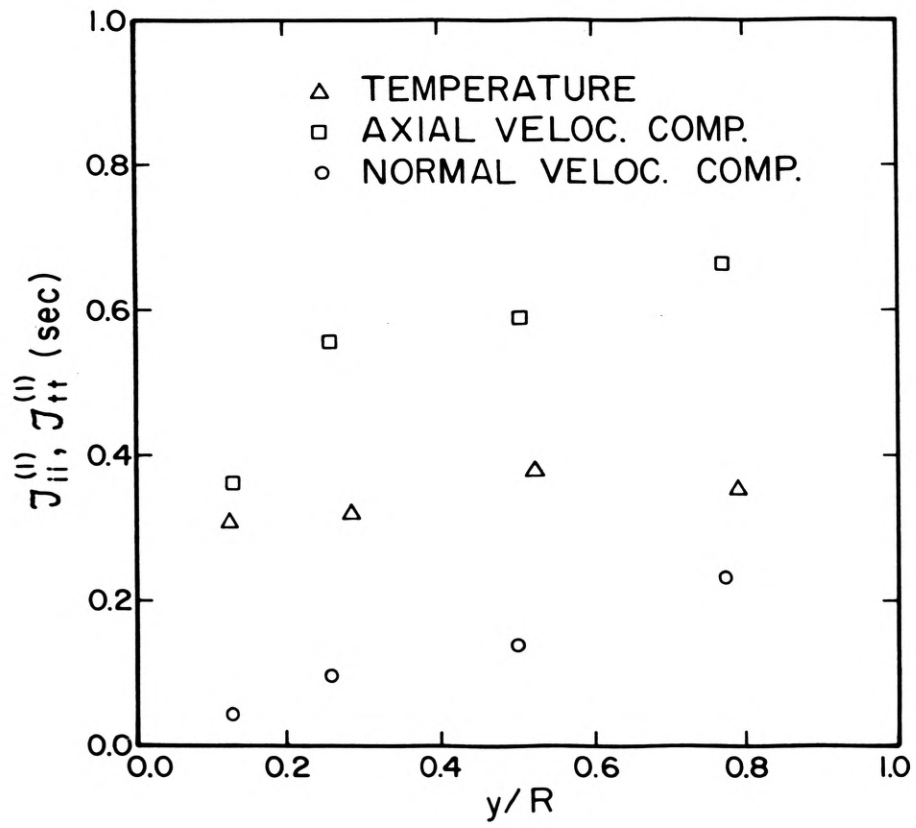


Figure D: Integral Convected Time Scales for Velocity Components and Temperature Fluctuations in Turbulent Pipe Flow.